

Statistical properties of color matching functions

María da Fonseca^{1, 2, 3} and Inés Samengo¹

¹Instituto Balseiro, CONICET, and Department of Medical Physics, Centro atómico Bariloche, Argentina.

³Center for Brain and Cognition, and Department of Information and Communication Technologies, Universitat Pompeu Fabra, Barcelona, Spain.

Keywords: Photon absorption, color perception, color matching functions.

Abstract

In trichromats, color vision entails the projection of an infinite-dimensional space (the one containing all possible electromagnetic power spectra) onto the 3-dimensional space determined by the three types of cones. This drastic reduction in dimensionality gives rise to metamerism, that is, the perceptual chromatic equivalence between two different light spectra. The classes of equivalence of metamerism is revealed by color-matching experiments, in which observers equalize a monochromatic target stimulus with the superposition of three light beams of different wavelengths (the *primaries*) by adjusting their intensities. The linear relation between the color matching functions and the absorption probabilities of each type of cone is here used to find the collection of primaries that need to be chosen in order to obtain quasi orthogonal, or alternatively, almost-always positive, color-matching functions. Moreover, previous studies have shown that there is a certain trial-to-trial and subject-to-subject variability in the color matching functions. So far, no theoretical description has been offered to explain the trial-to-trial variability, whereas the sources of the subject-to-subject variability have been associated with individual differences in the properties of the peripheral visual system. Here we explore the role of the Poissonian nature of photon capture on the wavelength-dependence of the trial-to-trial variability in the color matching functions, as well as their correlations.

Color vision has limitations. If we are instructed to provide objective measures of the percept produced by a chromatic stimulus, our responses are endowed with some degree of trial-to-trial variability. In a previous paper (da Fonseca and Samengo, 2016), we showed that although there are many putative sources of variability in the visual pathway, the Poissonian nature of photon absorption by cones suffices to explain a large fraction of the variance in discrimination experiments (MacAdam, 1942). Those experiments reported the trial-to-trial fluctuations in color-matching experiments in some of the popular systems of coordinates employed to report color, as well as in a so-called “natural” system (da Fonseca and Samengo, 2018). In this letter, we derive the effect of photoreceptor Poisson noise in the color-matching functions (CMFs). These functions are extensively used in colorimetry to represent color (see below). Quite unfortunately, the scientific community working in color, and often dealing with the needs of industry, only seldom talk to and are addressed by neuroscientists studying vision, more focused on principled descriptions. Our analytical description of the trial-to-trial variability of CMFs based on a probabilistic description of cone functioning is an attempt to facilitate the dialogue between the two fellowships.

When a light beam of spectrum $I(\lambda)$ impinges on the retina, the three types of color-sensitive photoreceptors, cones of type S , M and L absorb $\mathbf{k} = (k_s, k_m, k_\ell)^t$ photons with probability distribution (Zhaoping et al., 2011)

$$P[\mathbf{k}|I(\lambda)] = \prod_{i \in \{s, m, \ell\}} \text{Poisson}(k_i | \alpha_i), \quad (1)$$

where each Poisson factor reads

$$\text{Poisson}(k|\alpha) = e^{-\alpha} \frac{\alpha^k}{k!},$$

with mean and variance

$$\alpha_i = \beta_i \int I(\lambda) q_i(\lambda) d\lambda, \quad i \in \{s, m, \ell\}. \quad (2)$$

Here, the parameters β_i represent the fraction of each type of cone in the retina of the observer, and the curves $q_i(\lambda)$ are the cone fundamentals describing the wavelength dependence of the absorption probability of each type. The space of all possible light

spectra is hence projected on the 3-dimensional space spanned by the vector \mathbf{k} . Importantly, the projection is probabilistic, and in different trials, the same spectrum $I(\lambda)$ may generate different \mathbf{k} -vectors. The mean value of the number of absorbed photons of each type is $\langle \mathbf{k} \rangle = \boldsymbol{\alpha} = (\alpha_s, \alpha_m, \alpha_\ell)^t$.

Equation 2 not only provides an algorithm with which to calculate the mean and variance of the distribution of Eq. 1, but also constitutes a linear projection that transforms a spectrum $E(\lambda)$ into the triplet $\boldsymbol{\alpha}$. Thus interpreted, Eq. 2 provides the *LMS* color coordinates (Wyszecki and Fielder, 1971).

Nowadays, neuroscientists studying vision know that the only signal that reaches the brain carrying chromatic information is a function of the vector \mathbf{k} . Consequently, the filtering operation produced by cones is always present in our description of behavioral experiments. Yet, long before photoreceptors were described, Hermann von Helmholtz explored the psychophysics of color vision (von Helmholtz, 1910), and arrived to the conclusion that any chromatic sensation can be perceptually equated with a combination of three monochromatic beams of adjustable intensity, the so-called *primary colors*. The triplet of primaries is not unique, since many choices can be used, as long as the mixture two of the colors does not produce the chromatic sensation of the third.

In the 19th century, Hermann Grassmann (Grassmann, 1853) introduced the laws that carry his name, and govern the rules of color matching: symmetry, transitivity, proportionality and additivity (Wyszecki and Stiles, 2000). In 1931, the Commission internationale de l'éclairage (CIE) reported the results for a collection of the experiments called *color matching experiments* (Commission Internationale de l'Eclairage, 1932). Subjects were instructed to adjust the gains g_1, g_2, g_3 of three monochromatic beams of wavelengths $\lambda_1, \lambda_2, \lambda_3$ and intensities I_1, I_2, I_3 (the primaries) to match a *target* spectral color of wavelength λ_t . The experimenter showed a bipartite field on a screen. One of the halves was illuminated with the target stimulus, of spectrum

$$I_t(\lambda) = I_t \delta(\lambda - \lambda_t), \quad (3)$$

and the other half displayed the *matched* color, of spectrum

$$I_m(\lambda) = g_1 I_1 \delta(\lambda - \lambda_1) + g_2 I_2 \delta(\lambda - \lambda_2) + g_3 I_3 \delta(\lambda - \lambda_3). \quad (4)$$

The values of g_1, g_2 and g_3 were collected from 18 subjects, for a set of target wavelengths $\lambda_t \in [380 \text{ nm}, 780 \text{ nm}]$ every 5 nm. The population mean of each $g_i(\lambda_t)$ was defined as the red, the green and the blue *color matching functions* (CMF) of the so-called “standard observer” of Fig. 1A (Wyszecki and Stiles, 2000).

The CIE 1931 chose primaries of wavelength $\lambda_1 = 700 \text{ nm}$, $\lambda_2 = 546.1 \text{ nm}$ and $\lambda_3 = 435.8 \text{ nm}$. For λ_t between 430 and 550 nm no gains (g_1, g_2, g_3) could achieve a perceptual match. If, however, the red primary was added to the target spectrum with a specific intensity g_3 , observers were able to find positive gains g_1 and g_2 to achieve the match. By convention, then, the CMF evaluated at the target wavelength λ_t were defined by the gains ($g_1, g_2, -g_3$). The negative sign of the last component indicates that the beam of wavelength λ_3 was added to the target field (as opposed to the matched field) with gain g_3 .

A match between the perceived target and constructed colors implies that the probability distributions $P(\mathbf{k}|\boldsymbol{\alpha})$ of both beams coincide. The only way of achieving this equality is by inserting Eqs. 3 and 4 into Eq. 2, and obtaining exactly the same triplet ($\alpha_s, \alpha_m, \alpha_\ell$). Therefore, the gains g_1, g_2, g_3 must be chosen so that (Brainard and Stockman, 2010)

$$\sum_{j \in \{1,2,3\}} g_j I_j q_i(\lambda_j) = I_t q_i(\lambda_t), \quad \forall i \in \{s, m, \ell\}. \quad (5)$$

The parameters β_i describing the composition of the retina of the observer (Eq. 2) are cancelled out, so they do not appear in Eq. 5. As a consequence, the gains g_j chosen by observers with different retinas coincide.

The linear relation of Eq. 5 between the column vector $\mathbf{g} = (g_1, g_2, g_3)^t$ of the gains and the column vector $\mathbf{t} = (q_s(\lambda_t), q_m(\lambda_t), q_\ell(\lambda_t))^t$ of the target stimulus can be shortened by defining the matrix Q with entries

$$Q_{ij} = q_i(\lambda_j), \quad \text{with } i \in \{s, m, \ell\} \text{ and } j \in \{1, 2, 3\}$$

and the diagonal matrix D with entries

$$D_{jj} = \frac{I_j}{I_t}.$$

The change of base matrix

$$C = Q \cdot D \tag{6}$$

then relates \mathbf{g} and \mathbf{t} :

$$C\mathbf{g} = \mathbf{t}.$$

This equation can be solved uniquely for \mathbf{g} for all non-singular C matrices, yielding

$$\mathbf{g} = C^{-1} \mathbf{t}. \tag{7}$$

The requirement of a non-singular C is met by all triplets of non-coinciding primaries, as long as D is invertible, that is, none of the beams is turned off. If two primaries, however, are close to each other, the matrix C is close to singular, and one of its eigenvalues is close to zero. Unrealistically large gains g_j may then be required. If less than three primaries are used, then C is a rectangular matrix with more rows than columns, and cannot be inverted, implying that no match can be found. If, instead, more than three primaries are employed, C is a rectangular matrix with more columns than rows, and the system has infinite solutions. One of the primaries can be obtained by combination of the remaining three, so whichever gain is assigned to that primary, could also have been distributed among the other three.

Since the vector \mathbf{t} depends on the wavelength λ_t of the target beam, Eq. 7 relates the CMFs $g_j(\lambda_t)$ to the spectral selectivity of the photon absorption process (through Q), and the properties of the three chosen primaries (through the wavelengths $(\lambda_1, \lambda_2, \lambda_3)$ and the associated intensities (I_1, I_2, I_3) appearing in D). Hence, the three CMFs are linear combinations of the cone fundamentals $q_i(\lambda_t)$, and the coefficients of the linear combination, which depend on the three chosen primaries, define the change-of-base matrix C .

Figure 1A displays the original CMF reported by the CIE 1931, with the prediction

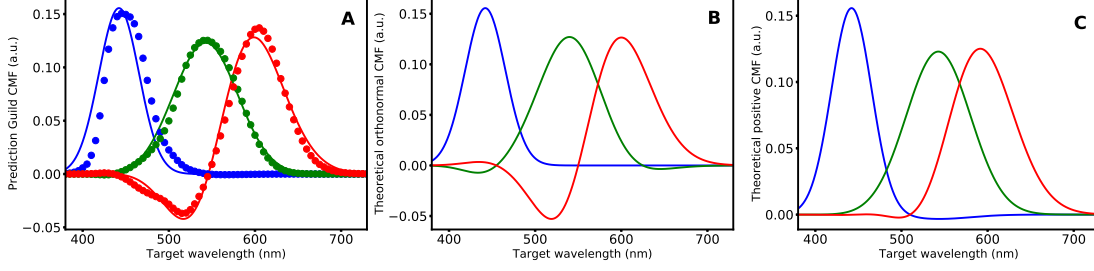


Figure 1: A: Color matching functions reported by Guild (Guild, 1932), employed by the CIE 1931 to construct their RGB and XYZ color spaces ($\lambda_1 = 435.8$ nm in blue dots, $\lambda_2 = 546.1$ nm in green dots and $\lambda_3 = 700$ nm in red dots) normalized to unit Euclidean norm, and the corresponding normalized theoretical prediction in solid lines (Eq. 7 calculated with the cone fundamentals of Stockman and Sharpe (2000)). B: Predicted normalized CMF corresponding to primaries $\lambda_1 = 455$ nm (blue), $\lambda_2 = 550$ nm (green), $\lambda_3 = 625$ nm (red), selected to minimize the scalar product between the curves. C: Predicted normalized CMF corresponding to primaries $\lambda_1 = 380$ nm (blue), $\lambda_2 = 510$ nm (green), $\lambda_3 = 775$ nm (red), selected to maximize the range of λ_t values for which the curves are positive.

for $g_i(\lambda_t)$ of Eq. 7, with $i \in \{1, 2, 3\}$. The diagonal elements I_i/I_t of matrix D were set to unity, which yields CMFs of unit Euclidean norm.

If instead of combining three monochromatic primaries, matching experiments are performed with light beams of arbitrary spectra $e_1(\lambda)$, $e_2(\lambda)$, $e_3(\lambda)$, the gains $g_j(\lambda_t)$ are still given by Eq. 7, but with a matrix Q with elements $Q_{ij} = \langle q_i, e_j \rangle$. The resulting CMF $g_j(\lambda_t)$ can still be obtained, and they still represent the gains of the three beams.

So far, the target beam was assumed to be monochromatic. If this restriction is relaxed, the spectrum $I'_t(\lambda)$ can be an arbitrary (non-negative) function. The linearity of Grassman's laws implies that the three gains (g'_1, g'_2, g'_3) required to achieve the match are linear combinations of the CMFs obtained for monochromatic targets, that is,

$$g'_j = \int g_j(\lambda) I'_t(\lambda) d\lambda, \quad (8)$$

where $g_j(\lambda)$ are given by Eq. 7. The values g'_1, g'_2, g'_3 are the “tri-stimulus values” of the beam I'_t , and constitute one possible system of coordinates in which the chromaticity of $I'_t(\lambda)$ is represented. Different choices of primaries result in different coordinate systems, since they yield different CMFs.

When the choice of primaries is only meant to produce CMFs that define a coordinate system (that is, whenever the actual execution of the color matching experiment is not required) unattainable primaries, often termed *imaginary* primaries, may be employed. Imaginary primaries are defined by power spectra that contain negative values, and therefore, cannot be instantiated in reality. Such is the case, for example, of the primaries that underlie the *LMS*, the *RGB* and the *YXY* coordinate systems.

Equation 8 implies that the tri-stimulus values are the projection of the target spectrum I'_t on the CMFs. Within this framework, the CMFs act as a base of the subspace of spectra that trichromats perceive. The first goal of this paper is to reveal two triplets of primary colors that produce CMFs that are particularly convenient.

The choice of the first triplet is guided by the requirement of obtaining CMFs that are as orthogonal as possible. Coordinate systems constructed with orthogonal bases are desirable, since correlations in the resulting tri-stimulus values reflect correlations in the original spectra, as opposed to correlations in the chosen base.

The color matching functions reported by the CIE 1931 were not far from orthogonal. The scalar products of the normalized version of those curves were $\langle g_1, g_2 \rangle = 0.018$, $\langle g_2, g_3 \rangle = 0.044$, and $\langle g_3, g_1 \rangle = -0.015$, where the sub-indices 1, 2, 3 refer to the primaries with wavelengths 435.8, 546.1 and 700 nm, respectively. The scalar products are small, but they can still be improved by diminishing $\langle g_2, g_3 \rangle$.

The search for primaries that produce orthogonal CMFs has been undertaken before (Thornton, 1999; Brill and Worthey, 2007; Worthey, 2012), by finding a linear transformation of some set of previously reported CMFs. However, the resulting primaries were imaginary. To produce an (almost) orthogonal base that is connected to a realizable color-matching experiment, here we performed an exhaustive numerical search of all triplets of monochromatic primaries between 380 and 775 nm, in steps of 5 nm., calculated their CMFs through Eq. 7, and retained the triplet that minimized the function $\langle g_1, g_2 \rangle^2 + \langle g_2, g_3 \rangle^2 + \langle g_3, g_1 \rangle^2$. The optimal triplet was $\lambda_1 = 455$ nm,

$\lambda_2 = 550$ nm, and $\lambda_3 = 625$ nm. The main difference with the CIE 1931 primaries is that the wavelength of the red beam is diminished. The resulting CMFs are displayed in Fig. 1B, and the most noticeable difference with the CMFs of CIE 1931 is that g_2 contains larger negative regions flanking both sides of its maximum, thereby diminishing the overlap with g_1 . The inner products between the resulting CMFs are $\langle g_1, g_2 \rangle = 0.012$, $\langle g_2, g_3 \rangle = 0.011$, $\langle g_3, g_1 \rangle = -0.01$.

In the second place, we search for primaries that produce CMFs with maximal domain of positive values. Such primaries are the optimal choice when attempting to construct metamers of monochromatic beams with the largest possible range of target wavelengths, since the negative portion of CMFs reflect a failure to construct the target percept. This request is relevant, for example, when choosing the LEDs of computer screens.

Again, we performed a numerical, exhaustive search of monochromatic primaries, and maximized the sum of the domains where the resulting CMFs were positive. The optimal triplet had wavelengths $\lambda_1 = 380$ nm, $\lambda_2 = 510$ nm, and $\lambda_3 = 775$ nm. In this case, the wavelengths are more separated from one another than in the original CIE 1931 primaries, and reached the minimal and maximal values employed in our search. Clearly, if no restriction is imposed on the amplitude of the gains, even more separated primaries would produce still more positive CMFs, since cones of different type would never be activated simultaneously. The normalized CMFs obtained with our search algorithm are displayed in Fig. 1C. Negative values could not be avoided for g_1 and g_3 , but the reached values were small (-0.003 and -0.002 , respectively), so it may be hypothesized that for those wavelengths, replacing a negative gain by zero would produce a minimal perceptual shift.

We now turn to the second goal of this paper, namely, to provide a principled derivation of the trial-to-trial variability and correlation structure of the CMFs, capturing the dispersion and the structure of the observer's responses. In our derivation, the source of variability is the stochastic nature of photon absorption (Eq. 1). We are aware of the ex-

istence of additional sources of variability. Still, here the aim is to assess how much of the experimental variability can be accounted for, taking only the stochasticity of photon absorption of Eq. 1 into account. The advantage of describing photon absorption alone, is that the probability distribution of Eq. 1 can be derived from first principles (da Fonseca and Samengo, 2016).

We interpret the matching experiment as the observer’s attempt to estimate the tri-stimulus values of the target stimulus. In other words, if the coordinates of the target monochromatic stimulus obtained from Eq. 7 are (g_1, g_2, g_3) , the behavioral response obtained in the color matching task in a single trial $\hat{\mathbf{g}} = (\hat{g}_1, \hat{g}_2, \hat{g}_3)^t$ can be interpreted as an estimator of the true \mathbf{g} performed by the subject from the absorbed photons $\mathbf{k} = (k_s, k_m, k_\ell)^t$. The trial-to-trial fluctuations of $\hat{\mathbf{g}}$ are captured by the 3×3 mean quadratic error matrix E of entries

$$E_{ab}(\mathbf{g}) = \langle [\hat{g}_a(\mathbf{k}) - \langle \hat{g}_a \rangle] [\hat{g}_b(\mathbf{k}) - \langle \hat{g}_b \rangle] \rangle,$$

where the brackets represent an expectation value weighted with $P(\mathbf{k}|\mathbf{g})$. The diagonal elements of E_{jj} represent the variances of the measured g_i values, and the off-diagonal elements E_{ab} , the covariances.

The Crámer-Rao bound (Rao, 1945; Cramér, 1946; Cover and Thomas, 2012) states that the mean quadratic error E of any unbiased estimator is bounded from below by the inverse of the Fisher Information $J(\mathbf{g})$, a 3×3 matrix of entries

$$J_{ab}(\mathbf{g}) = - \left\langle \frac{\partial^2 \ln P(\mathbf{k}|\mathbf{g})}{\partial g_a \partial g_b} \right\rangle. \quad (9)$$

The Fisher Information matrix is the metric tensor with which infinitesimal distances in color space can be calculated, such that traversing a unit of distance in color space modifies the distribution of \mathbf{k} vectors in a fixed amount (Amari and Nagaoka, 2000). The bound reads

$$E \cdot J \geq \mathbb{1}, \quad (10)$$

and states that all the eigenvalues of the matrix product $E \cdot J$ must be larger or equal than unity. It implies that inasmuch as J is associated to the notion of information, J^{-1}

is associated to the notion of minimal mean quadratic estimation error. The larger the information, the smaller the error, and vice versa. The fact that Eq. 10 is expressed in matrix form means that the bound is directional. In other words, the mean quadratic error may take different values along different directions: Along the eigenvectors of E , the error is equal to the corresponding eigenvalues. Equation 10 is only valid for unbiased estimators, that is, those for which $\langle \hat{\mathbf{g}}(\mathbf{k}) \rangle = \mathbf{g}$. A more complex formula is required in the biased case (Cover and Thomas, 2012). However, if the stimulus is not surrounded by a chromatic background (and such is the case of the color matching experiment discussed here), behavioral errors have zero mean (Klauke and Wachtler, 2015, 2016), so we work under the assumption that the nervous system is able to implement at least one unbiased estimator.

Equation 10 is an inequality, so the Fisher Information can be employed to bound, but not to calculate, the mean quadratic error. Even so, in this paper we assume that the equality holds, and derive the mean quadratic error analytically as

$$E \approx J^{-1}, \quad (11)$$

since J can be obtained analytically from Eqs. 9 and 1. The assumption is only valid if all subsequent processing stages, downstream from photon absorption, preserve the information encoded by the vector \mathbf{k} . In 2016, we showed that the mean quadratic error obtained by assuming that the equality holds captures 87% of the variance of behavioral discrimination experiments (da Fonseca and Samengo, 2016). Assuming the equality, hence, seems to be justified up to a reasonable degree. Continuing with this line of thought, we here explore the consequences of this assumption in the mean quadratic error of behavioral matching experiments.

The Fisher Information matrix was obtained in da Fonseca and Samengo (2016), in the LMS coordinate system, obtaining a diagonal matrix of entries

$$J(\boldsymbol{\alpha})_{ab} = \frac{1}{\alpha_a} \delta_{ab}, \quad (12)$$

where δ_{ab} is the Kronecker delta symbol. To predict the trial-to-trial fluctuations in matching experiments, this tensor must be transformed to the \mathbf{g} coordinate system. To

that end, we define the diagonal matrix B with entries

$$B_{ij} = \beta_i \delta_{ij},$$

containing the fractions β_i of each type of cones. The coordinate transformation between α and \mathbf{g} is

$$\alpha = B \cdot C \mathbf{g}. \quad (13)$$

Consequently, the transformation rule for the metric tensor is (da Fonseca and Samengo, 2016)

$$J(\alpha) = (B \cdot C)^t \cdot J(\mathbf{g}) \cdot (B \cdot C). \quad (14)$$

Inserting Eq. 12 into Eq. 14, using the expression 13, and solving for $J(\mathbf{g})$, the Fisher Information can be obtained analytically,

$$J(\mathbf{g})_{ab} = I_a I_b \sum_{i \in \{s,m,\ell\}} \frac{\beta_i q_i(\lambda_a) q_i(\lambda_b)}{\sum_{j=1}^3 q_i(\lambda_j) I_j g_j}. \quad (15)$$

If the color-matching experiment is performed with monochromatic target stimuli (Eq. 3), the Fisher Information matrix of Eq. 15 reduces to

$$J(\mathbf{g})_{ab} = \frac{I_a I_b}{I_t} \sum_{i \in \{s,m,\ell\}} \frac{\beta_i q_i(\lambda_a) q_i(\lambda_b)}{q_i(\lambda_t)}. \quad (16)$$

The Fisher Information matrix bears an explicit dependence on $(\beta_s, \beta_m, \beta_\ell)$, implying that observers with different retinal composition respond with trial-to-trial fluctuations of varying structure. Moreover, writing the intensities (I_1, I_2, I_3) in units of I_t reveals that the Fisher Information is linear in the target intensity I_t . Therefore, the variance of the responded g_j is inversely proportional to the total light intensity employed in the experiment.

The Fisher Information matrix of Eq. 16 can be inverted to yield the mean quadratic error under the assumption of Eq. 11. In Fig. 2A, the diagonal elements E_{aa} are displayed (the variances), for a retinal composition of $\beta_s = 0.05, \beta_m = 0.45, \beta_\ell = 0.5$, which is quite typical for human trichromats. We also verified that modifying these values within the physiological range produced only minor changes in the derived variances and covariances. The ratios I_j/I_t were set to unity, in order for the resulting

CMFs to have unit norm. The global scaling factor I_t was set to 0.014, in order for the maximum of the variance in g_3 (peak of the red curve in Fig. 2A) to equate the experimental height (Fig. 2C, see below).

The off-diagonal elements E_{ab} can be seen in Fig. 2B, showing that all correlations are negative, and they tend to be particularly significant in those regions of the spectrum where the two corresponding CMFs overlap. Negative correlations imply that if, in one particular trial, the observer sets one of the gains above average, they are likely to set the other two below average, at least, if there is an overlap between the corresponding CMFs.

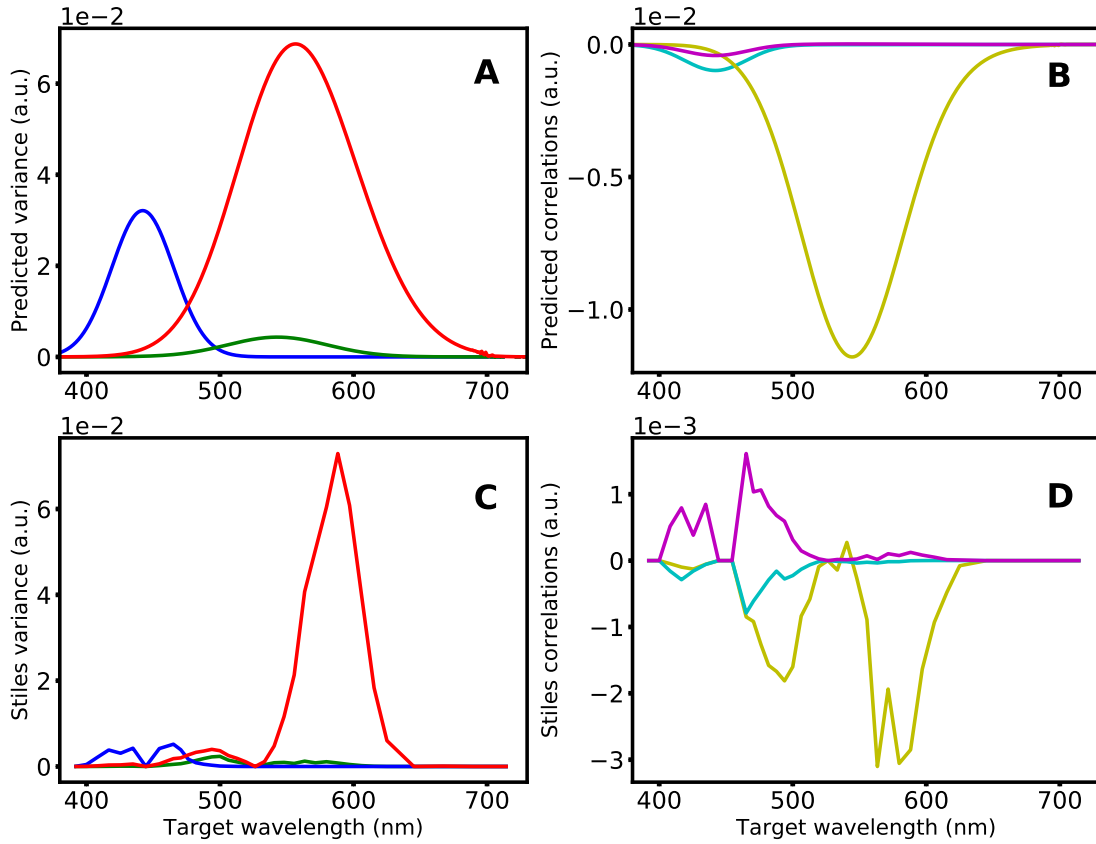


Figure 2: A: Normalized theoretical prediction for the variance of the CMFs of Fig. 1A, as a function of the target wavelength λ_t . The three curves are the diagonal terms of the inverse of the matrix in Eq. 16. B: Correlations between the CMFs, obtained from the off-diagonal terms of the inverse of the matrix in Eq. 16. C and D: Variances and correlations obtained from multiple subjects performing the color-matching experiment (Stiles and Burch, 1959)

Some previous studies have addressed the subject-to-subject variability of color-matching experiments (Stiles and Burch, 1959; Wyszecki and Fielder, 1971; Alfvén and Fairchild, 1997; Fairchild and Heckaman, 2013, 2016; Asano et al., 2016a,b; Emery et al., 2017; Murdoch and Fairchild, 2019; Emery and Webster, 2019), and only a few have explored the trial-to-trial variability of the responses of a single subject (Wyszecki and Fielder, 1971; Alfvén and Fairchild, 1997; Sarkar et al., 2010; Asano, 2015). The two types of variability derive from different sources. Subject-to-subject variability is mainly due to individual differences in biophysical and physiological properties, and describes the degree of agreement in the percept produced by a given stimulus in a population of observers. Trial-to-trial variability, instead, reflects the inherent uncertainty with which a given observer perceives a given stimulus, and stems from noisy processes both outside and inside the visual system.

The inter-subject variability, has been more exhaustively characterized, probably for commercial purposes, and can be depicted as a function of wavelength (Fig. 2C and D). Theoretical studies (Fairchild and Heckaman, 2013; Asano, 2015; Asano et al., 2016a; Murdoch and Fairchild, 2019) on the inter-subject variability take into account individual differences in lens and macular pigment density, retinal composition (matrix B), and variations in the shape of the cone fundamentals $q_s(\lambda)$, q_m and $q_\ell(\lambda)$. Experimental data with the CMFs of a population of 49 subjects (Stiles and Burch, 1959) are available online (Fig. 2C and D).

Unfortunately, we lack experimental data on the trial-to-trial fluctuations of a single observer, at least, beyond crude estimation performed with very few samples. The results of Wyszecki and Fielder (1971) are difficult to interpret, since the variability of a single subject in different sessions (separated by several weeks or months) is considerably larger than one obtained in a single session of multiple trials, suggesting that some experimental conditions may have changed from one session to the next. Experiments estimating the intra-observer variability from 3 matches performed by each subject were published in the PhD Dissertation of Yuta Asano (2015). This trial-to-trial variability was approximately half the inter-observer variability, in accordance

with earlier estimations (Alfvin and Fairchild, 1997; Sarkar et al., 2010). Importantly, the variability was estimated for a collection of non-monochromatic target colors, so it cannot be displayed as a function of the target wavelength.

To our knowledge, the present study is the first analytical derivation of the trial-to-trial variability of the CMFs, deduced from one well identified source of noise: The Poissonian nature of photon absorption. The result can be displayed as a function of the target wavelength (Fig. 2A and B). Since our results cannot be reliably compared with experimental data recorded with multiple trials in a single observer, we compare them with those obtained with a single trial of multiple observers, understanding that differences are expected, due to the diverse sources of variability.

The experimental result of the population variances exhibit a marked peak for the red primary (Fig. 2C), the position of which was fairly well reproduced by the theoretical variance for a single observer (Fig. 2A). Therefore, part of the variance reported in the experimental result could potentially stem from intra-subject variability. The experimental variances of the other two primaries (red and blue curves in Fig. 2A) are too noisy to be useful. However, the relative size of the blue curve (compared to the red) in the theoretical result does not coincide with the experimental relation. Therefore, the population variability present in Fig. 2C and absent from Fig. 2A probably affects differentially the two primaries. No conclusions can be drawn about the absolute magnitude of the theoretical and experimental curves, since the analytical result contains a global scale factor I_t , which was fixated in Fig. 2A and B only to draw the variances.

The experimental covariances of the gains are also noisy (Fig. 2D). Both the theoretical and experimental covariances become significantly different from zero in those regions of the spectrum where the corresponding CMFs overlap. The theoretical result captures the sign of the (negative) covariance for the green-red interaction (yellowish curves) and the blue-green interaction (cyan), but not for the blue-red case (magenta). This discrepancy implies that, at least in the case of the blue-red interaction, either (a) subject-to-subject variability, or (b) additional stochasticity in downstream processing

stages of a single subject, play an important role in the co-variation of g_1 and g_3 .

In summary, in this letter we presented a theoretical derivation of the variances and co-variances expected in color-matching experiments when the sole source of noise is the stochasticity inherent to Poissonian photon absorption by cones. We were not able to find experimental data on intra-subject variability of CMFs obtained for monochromatic target stimuli, so we hope that the present study motivates psychophysical experiments. If the measured variances and covariances coincide with the analytical result obtained here, photoreceptor noise may be concluded to be a crucial ingredient in the perceptual variability of chromatic vision. Instead, if experiments happen to reveal a different behavior, subsequent stages in color processing may be concluded to play the lead.

Acknowledgements

This work was supported by Agencia Nacional de Investigaciones Científicas y Técnicas, Consejo Nacional de Investigaciones Científicas y Técnicas, Comisión Nacional de Energía Atómica and Universidad Nacional de Cuyo, all from Argentina.

References

- Alfvin, R. L. and Fairchild, M. D. (1997). Observer variability in metameric color matches using color reproduction media. *Color Research & Application*, 22(3):530–539.
- Amari, S. I. and Nagaoka, H. (2000). *Methods in information Geometry*. Oxford University Press, Oxford.
- Asano, Y. (2015). *Individual Colorimetric Observers for Personalized Color Imaging*, Ph.D. Dissertation. Munsell Color Science Laboratory, Rochester Institute of Technology.

- Asano, Y., Fairchild, M. D., and Blondé, L. (2016a). Individual colorimetric observer model. *PLoS ONE*, 11(2):1–19.
- Asano, Y., Fairchild, M. D., Blondé, L., and Morvan, P. (2016b). Color matching experiment for highlighting interobserver variability. *Color Research and Application*, 41(15):530–539.
- Brainard, D. H. and Stockman, A. (2010). Colorimetry. In *The Optical Society of America Handbook of Optics, Volume III: Vision and Vision Optics*. McGraw Hill.
- Brill, M. H. and Worthey, J. A. (2007). Color matching functions when one primary wavelength is changed. *Color Research & Application*, 32(1):22–24.
- Commission Internationale de l’Eclairage (1932). *Proceedings 1931*. Cambridge University Press, Cambridge.
- Cover, T. M. and Thomas, J. A. (2012). *Elements of information theory*. John Wiley & Sons.
- Cramér, H. (1946). A contribution to the theory of statistical estimation. *Scandinavian Actuarial Journal*, 1946(1):458–463.
- da Fonseca, M. and Samengo, I. (2016). Derivation of human chromatic discrimination ability from an information-theoretical notion of distance in color space. *Neural Computation*, 28(12):2628–2655.
- da Fonseca, M. and Samengo, I. (2018). Novel perceptually uniform chromatic space. *Neural Computation*, 30(6):1612–1623. PMID: 29566354.
- Emery, K. J., Volbrecht, V. J., Peterzell, D. H., and Webster, M. A. (2017). Variations in normal color vision. vi. factors underlying individual differences in hue scaling and their implications for models of color appearance. *Vision Research*, 141:51–65.
- Emery, K. J. and Webster, M. A. (2019). Individual differences and their implications for color perception. *Current Opinion in Behavioral Sciences*, 30:28 – 33. Visual perception.

- Fairchild, M. D. and Heckaman, R. L. (2013). Metameric observers: A monte carlo approach. *Color and Imaging Conference*, 2013(1):185–190.
- Fairchild, M. D. and Heckaman, R. L. (2016). Measuring observer metamerism: The nimeroff approach. *Color Research & Application*, 41(2):115–124.
- Grassmann, H. (1853). Zur theorie der farbenmischung. *Annalen der Physik und Chemie*, 165(5):69–84.
- Guild, J. (1932). The colorimetric properties of the spectrum. *Philosophical Transactions of the Royal Society of London A*, 230(681–693):6149–187.
- Klauke, S. and Wachtler, T. (2015). “tilt” in color space: Hue changes induced by chromatic surrounds. *Journal of Vision*, 15(13):1–11.
- Klauke, S. and Wachtler, T. (2016). Changes in unique hues induced by chromatic surrounds. *Journal of the Optical Society of America*, 33(3):A255–A259.
- MacAdam, D. L. (1942). Visual sensitivities to color differences in daylight. *Journal of the Optical Society of America*, 32(5):247–274.
- Murdoch, M. J. and Fairchild, M. D. (2019). Modelling the effects of inter-observer variation on colour rendition. *Lighting Research & Technology*, 51(1):37–54.
- Rao, C. R. (1945). Information and the accuracy attainable in the estimation of statistical parameters. *Bulletin of the Calcutta Mathematical Society*, 37:81–89.
- Sarkar, A., Blondé, L., Le Callet, P., Autrusseau, F., Morvan, P., and Stauder, J. (2010). A color matching experiment using two displays: design considerations and pilot test results. *Conference on Colour in Graphics, Imaging, and Vision. Society for Imaging Science and Technology*, 2010(1):414–422.
- Stiles, W. S. and Burch, J. M. (1959). Npl colour-matching investigation: final report. *Journal of Modern Optics*, 6(1):1–26.
- Stockman, A. and Sharpe, L. T. (2000). Spectral sensitivities of the middle- and long-wavelength sensitive cones derived from measurements in observers of known genotype. *Vision Research*, 40(13):1711–1737.

- Thornton, W. A. (1999). Spectral sensitivities of the normal human visual system, color-matching functions and their principles, and how and why the two sets should coincide. *Color Research & Application*, 24(2):139–156.
- von Helmholtz, H. (1910). *Treatise on Physiological Optics*. Optical Society of America.
- Worthey, J. A. (2012). Vectorial color. *Color Research & Application*, 37(6):394–409.
- Wyszecki, G. and Fielder, G. H. (1971). New color-matching ellipses. *Journal of the Optical Society of America*, 61(9):1135–1152.
- Wyszecki, G. and Stiles, W. S. (2000). *Color Science: Concepts and Methods, Quantitative Data and Formulae*. Wiley Interscience, New York.
- Zhaoping, L., Geisler, W. S., and May, K. A. (2011). Human wavelength discrimination of monochromatic light explained by optimal wavelength decoding of light of unknown intensity. *PLoS ONE*, 6(5):e19248.